BioMEMS Wireless Pressure Sensor

Daniel V. Pearce, *Undergraduate Student, RIT Microe*

Abstract— **A design and manufacture of a wireless pressure sensor was proposed as a future tool for use in biological monitoring. This device is designed to acquire pressure changes through a change in capacitance. This is accomplished using a large circular parallel plate capacitor separated by a micron of air. The upper and lower plates are connected together via a large planar inductor on the opposite end of the device. The inductor and capacitor in a parallel form a resonant circuit with resonant frequency equal to one over the square root of inductance times capacitance. The resonant frequency can be dependent on both the inductance and capacitance changes. Since the inductance is fixed, the resonant frequency should change with respect to the capacitance. The capacitance will change as the pressure changes and therefore pressure can be measured through frequency.**

In the process of manufacturing this device, many unforeseen problems arose resulting in structural and design failures. These problems along with their discovered solutions will be addressed.

Index Terms—**BioMEMs, Capacitive Sensor, Pressure Sensor, Wireless**

I. Introduction [1]

Medical science has evolved much since the time when bleeding was performed regularly to keep illness away. Since that time, science has found new and better ways to monitor vitals and evaluate potential problems. Despite all the gains that have been made, there are still mistakes made. The methods of measuring something as simple as blood pressure often prove to be inaccurate or fallible. To quote, Dr. Dose, "A patient's blood pressure can be different depending on who is taking it". Statements like this, lead to the assumption that there must be a better way.

It is the consistent idea that everything can be improved that has led more recently to the pursuit of bioMEMS technology. BioMEMS are nothing more than MEMS (Micro Electro Mechanical Systems) that are being designed for introduction into a biological system. There are many hurdles in reaching this point.

The first and most important obstacle to overcome is that of size. The acronym of MEMS tries to depict the desired scale of such devices, but in truth, a lot of MEMS technology is closer to being on the millimeter scale. The limitation of such devices is that they can interfere with the operation of the system they are being introduced into. It is most desirable for such devices to be on the scale of a few microns. Fig 1 shows an example of a second-generation device designed around the turn of the century.

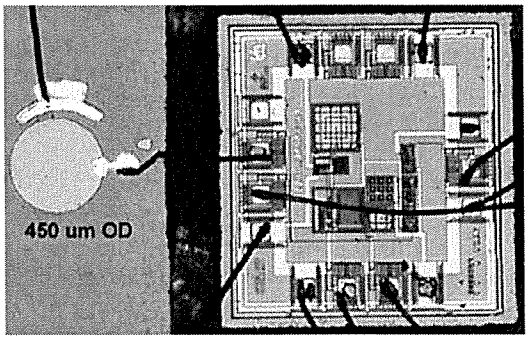

Fig 1. Example of an older scaled capacitive sensor. This device was used as part of a telemetry based, capacitive system for measurement of pressure changes. [2]

For the future, it will be necessary to reduce such devices in scale. Ideally, these devices would be smaller than any blood vessel in the body. This is reasoned based on the idea, that if an implanted device were to break free and end up in the blood stream, it would need to be small enough to not cause any damage.

II. Theory [1]

For a device to be implantable, a method of communication is necessary. The method looked at most commonly is that of resonant frequency transmission. Ref. [2] discusses the use of what it calls a passive telemetry link. This design makes use of an resonant frequency field to transfer energy to the implanted device, which is used to operate the pressure sensor. Fig 2 shows the basic schematic of this operational procedure.

Submitted May 22, 2006. This work was supported by the RIT Microe Department (sponsored by Dr. Lynn Fuller).

Daniel V. Pearce is an undergraduate student at Rochester Institute of Technology in the Microelectronic Engineering Program (phone: 585-734-7987; e-mail: dvp4799@rit.edu).

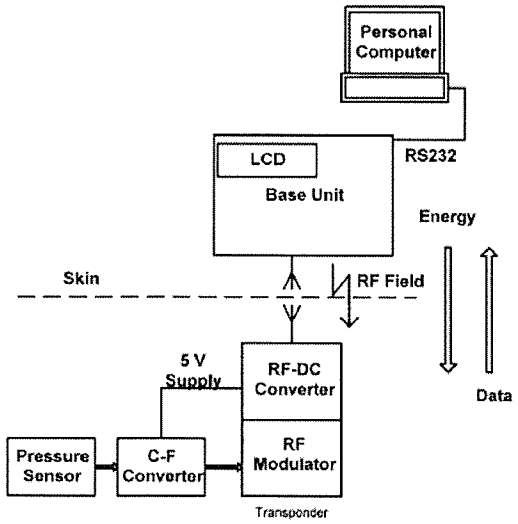

Fig 2. Pressure sensor telemetry system for implantation, a block diagram. This system is designed to interface with a isolated capacitive sensor. [2]

The following sets of equations involve the characterization of the telemetry link and the pressure sensor device. Data is transferred through the modulated resonant frequency absorption rate. This is then translated into an 8-bit unsigned byte array.

$$T = \frac{2C_x}{I_0}\left(V_{bias} - V_{TN}\right)\left(\sqrt{n} - 1\right) \qquad (1)$$

Equation (1) is used to determine the period of the output pulse. Where Cx is the sensor capacitance of the large area capacitance pressure sensor and n is the ratio of Ih to Il, high current to low current.

$$I_0 = k\frac{W_0}{L_0}\left(V_{\text{bias}} - V_{TN}\right)^2 \qquad (2)$$

Equation (2) depicts the standard relationship of saturation current in a transistor. k represents the mobility term, W0 is the initial width and L0 is the initial length. By inverting (1) and then substituting (2), the device frequency can be determined.

$$f = \frac{k\frac{W_0}{L_0}\left(V_{\text{bias}} - V_{TN}\right)}{2C_x\left(\sqrt{n} - 1\right)} \qquad (3)$$

The final equation (3) shows that frequency is independent of input voltage, but dependent through k and the threshold voltage on temperature.

The capacitance of a parallel plate capacitor, which operates through deflection modulation, has been characterized in (4).

$$C = \int_s \int \varepsilon_0 \left(\frac{1}{d - w(r)}\right) \qquad (4)$$

Where w(r) is the deflection of the diaphragm, d is the gap distance and ε0 is the permittivity of vacuum.

$$C = \int_0^{\alpha}\int_0^{2\pi} \frac{\varepsilon_0}{d - \frac{P\alpha^4\left[I_0\left(\frac{kr}{\alpha}\right) - I_0(k)\right]}{2k^3 I_1(k) D} - \frac{P\alpha^2\left(\alpha^2 - r^2\right)}{4k^2 D}} r dr d\theta \qquad (5)$$

Equation (5) depicts the finalized equation from (4) where the formulas for deflection, w(r), have been substituted.

$$D = D_0 h^3$$

$$D_0 = \frac{E}{12\left(1 - v^2\right)} \qquad (6)$$

$$k^2 = \frac{\sigma_i \alpha^2 h}{D}$$

α represents the plate radius, σi is the intrinsic stress, h the plate thickness, and I(k) is the modified Bessel function. Using a theoretical value of 1.42x1010 Pa for D0, the theoretical graph of pressure verses frequency as depicted in Figure 4 was plotted.

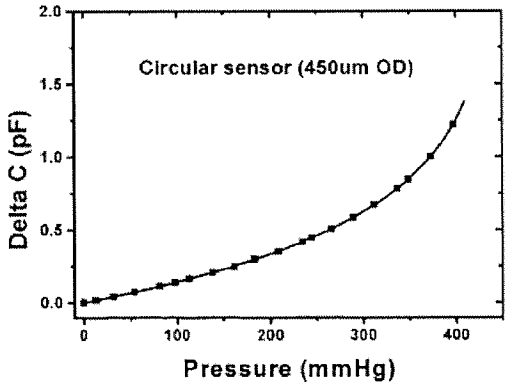

Fig 4. Theoretical pressure vs. frequency for the capacitive pressure sensor utilizing RF communication. [2]

III. Procedure

Processing is performed on four-inch wafers that were n-type doped. The wafers are then processed using Chemical Mechanical Processing (CMP) to polish the backside of the wafers. This is done due to the need for backside lithography. CMP is performed for 45 minutes using alkaline colloidal silica to achieve a mirror like finish. The wafers are then cleaned to remove any residual CMP particles.

A pad oxide of 500 Å is grown using dry oxidation to reduce stress on the subsequent nitride layer deposited on top of the oxide. A split occurred in nitride processing due to problems encountered. The first deposition was a 900 Å using a recipe titled "stoichiometric" nitride, which has a deposition rate of 20 Å/min at 800°C. The second split was a 1500 Å nitride deposition using a recipe titled "factory" nitride, which has a deposition rate of 75 Å/min. Table 1 depicts the recipe differences as documented by the RIT SMFL. The nitride is deposited using Chemical Vapor Deposition (CVD).

TABLE 1

	800C Stoich. Nitride	810C Factory Nitride
Actual Gas Flow (sccm)	10 DCS 200 NH_3	60 DCS 150 NH_3
Center ProfileTemperature	800C	810C
Pressure (mtorr)	300	400
Nominal Dep. Rate 4 inch	20 Å/min.	74 Å/min.

Photolithography level one is performed using a five-inch quartz plate for contact lithography. The lithography is performed on a KA-150 contact aligner. Shipley 1813 g-line resist is coated using the SVG automated coat and develop track. Lithography layer one is exposed on the backside of the wafer. Exposure requires 20 seconds using default tool positions for simplicity. Wafers are also developed on the SVG track.

A short buffered oxide etch (BOE) is then performed for 1 minute to remove any oxynitride from the opened areas. The nitride is etched using the LAM 490 plasma etch tool. The gas used is SF_6, which has the potential to etch the oxide and subsequently the substrate underneath. Nitride has a known etch rate of 629 Å/min and thermal oxide has an etch rate of 194 Å/min. Using endpoint detection utilizing wavelength intensity measurements, it is possible to determine when the nitride has been etched through.

A short BOE with an etch rate of oxide of 586 Å/min is used to strip the oxide followed by a resist strip. A potassium hydroxide (KOH) etch with an approximate etch rate of 1.2 μm/min, is performed for ~6 hours. This is to form for rectangular pits leaving approximately 50 μm of silicon. Due to the nature of KOH being a heavy metal that can cause contamination of other systems, a decontamination clean, that consists of hydrogen chloride and peroxide, is conducted for twenty minutes. Following this clean, a one-minute BOE is performed to strip any oxynitride that may have formed on the surface of the nitride. A hot phosphoric acid etch is done to remove the nitride with an etch rate for the factory recipe of 83 Å/min and for the stoichiometric recipe an etch rate of 116 Å/min.

A BOE is done next to remove the pad oxide and a 5000 Å wet oxide is grown to provide electrical isolation of the later metal layers from the substrate. Aluminum is then deposited using a physical vapor deposition (PVD) process on the CVC 601 sputter deposition system. The aluminum deposits around ~275 Å/min. Approximately 10,000 Å of aluminum is deposited over the front side of the wafer. Resist is then coated over the front side of the wafer using a manual hand spinner. Lithography level two is performed using backside alignment on the contact aligner. The wafers are inserted upside down with a drop of water to provide adhesion to the mask plate. Using the alignment microscopes to align the backside to the mask pattern, and then removing the mask with wafer attached and using the exterior alignment marks to align the second level mask to the front. The two layers are clamped together, the system is reset and then exposure occurs in a timed manner for 7 seconds.

Wafers are then developed using the hand develop spinner They are then etched in an aluminum etchant to transfer the image to the aluminum layer. The aluminum etchant etches a a rate of 2646 Å/min and therefore it is important to not over etch due to potential undercutting. A layer of 1 μm of plasma enhanced chemical vapor deposition (PECVD) called TEOS which is deposited using the P5000 deposition tool at a rate o about 100 Å/sec.

Photolithography layer three is the following step. Photo resist is again applied by hand as it will be for all remaining levels. This and all remaining layers are aligned through backside alignment or physical feature alignment on the surface. Photo layer three defines the contact cuts that will connect the first metal layer to the second. After development, the contact cuts are etched using BOE at an etch rate of 1440 Å/min for TEOS. The fourth level of lithography defines the actual diaphragm of the device. The resist is left after development; a 2 μm layer of aluminum is then deposited. Lithography layer five defines the second layer of metal. The aluminum is etched using wet chemistry, and then using acetone as a resist solvent, the resist is stripped from the surface and the diaphragm resist creating a 1 μm spaced capacitor pressure sensor.

8000 Å of TEOS is deposited to insulate the final metal layer. 3000 Å of aluminum are then deposited over the surface of the wafer. Photolithography layer six is then used to define an etch mask for the device isolation from the substrate. The aluminum is etched using wet chemistry and then the backside is thinned using plasma etching in the Drytek Quad. The wafer is then diced using a diamond wafer saw and then plasma etched again to completely define the outline of the device and then the aluminum is removed from the surface to begin testing.

IV. Results

During the first run, a major problem was encountered when the hard mask failed to protect the wafer surface from unwanted etch damage. The hard mask was the nitride layer deposited in the beginning of the processing. During the first run, the nitride that was deposited was the stoichiometric nitride, which appeared to have failed to provide the necessary protection. Fig 5 shows a picture of a broken wafer with etch holes through it from the KOH etch.

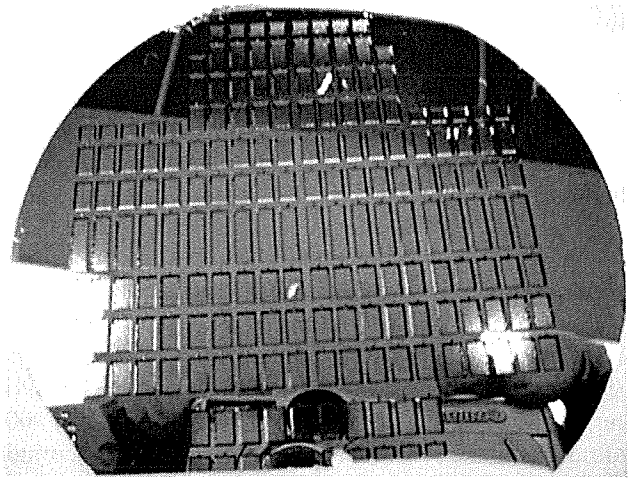

Fig 5. Wafer made brittle from KOH mask failure. Wafer flat has broken off.

The failure of the hard mask resulted in the breakage of the entire first batch of wafers. One of the major failures that occurred was that of an inability to maintain a vacuum seal on any wafers. Due to the use of vacuum technology in most tool systems, this made it difficult to continue processing following the completion of the KOH etch. For the second run, a different nitride recipe was used as mentioned in the procedure section. A thicker layer of nitride was also deposited. The comparison between the two recipes can be seen in Table 1.

A second run was performed. The previous issues were overcome, and processing was completed up to the third lithography layer. Another problem that was encountered was in fact a problem from the beginning. The mask layers were incorrectly manufactured and the first three layers consisted of one design, and the second of a different design. The second design was intended to be the final design, but miscommunication resulted in the wrong design being printed. As a result it was impossible to complete the processing.

Figs 6 and 7 show a comparison of images of photoresist on aluminum for two different exposure times. Fig 6 shows an exposure of 7 seconds and Fig 7 shows an exposure of 10 seconds. Figs 8 and 9 show the transferred image from the 7-second exposure. Fig 8 shows a zoomed out view at 25x of the features of the device and Fig 9 shows a 100x view of one of the inductor coils with 2 μm lines and 4 μm spaces.

Due to the incomplete nature of the project, no electrical testing or performance testing was completed in order to determine effectively the feasibility or practicality of this project. At this time, the operation of this device is entirely based on mathematics and theory.

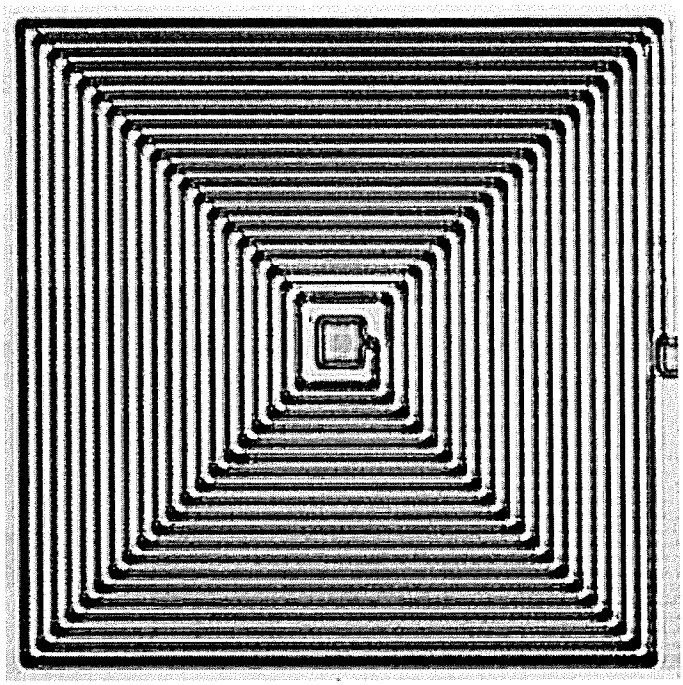

Fig 6. 2 μm lines and 4 μm spaces make up a planar inductor coil. Photoresist printed on aluminum. 7-second exposure.

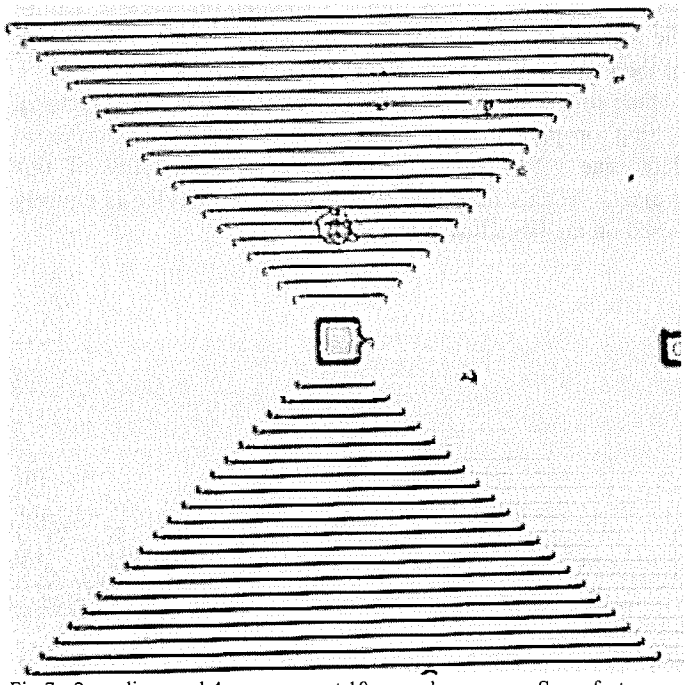

Fig 7. 2 μm lines and 4 μm spaces at 10-second exposure. Same features as the above figure Fig 6.

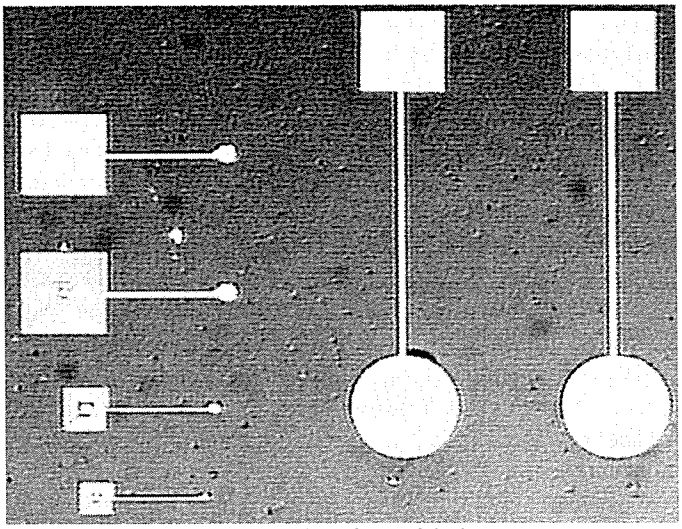

Fig 8. Aluminum on oxide. 25x view of several devices.

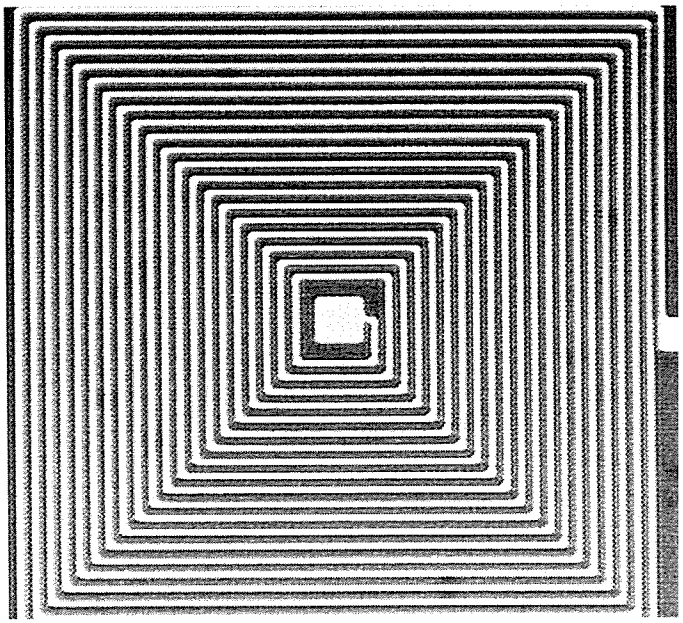

Fig 9. Aluminum on oxide, 100x view of 2μm lines and 4 μm spaces as in previous Figs 6 and 7 after transfer of pattern.

V. Conclusions

In conclusion, device processing was attempted two times and no success was forthcoming. The first attempt reached step 20 and the second attempt reached step 24 out of the 40 step device process. In the second attempt it was found that 7 seconds printed the best 2 μm lines, but based on processing techniques, 2 μm lines and 2 μm spaces could not be printed successfully. It was also determined that 1500 Å of nitride using the factory recipe formed a better hard mask than 900 Å of nitride using the stoichiometric recipe. Assuming a printing of the correct layers for mask plates one through three, then

third attempt to process these devices will be performed.

REFERENCES

[1] Daniel Pearce, "Biological Pressure Sensor Technology," Senior Design Review Paper, 2005.

[2] Stavros Chatzandroulis, Dimitris Tsoukalas, and Peter A. Neukomm, "A Miniature Pressure System with a Capacitive Sensor and a Passive Telemetry Link for Use in Implantable Applications," in *Journal of Microelectromechanical Systems*, 2000, Vol. 9, No. 1 p. 18.

Daniel V. Pearce born in Montpelier, France 1983. Bachelor's in Microelectronic Engineering graduated May 2006 and Master's in Material Science graduated August 2006 from Rochester Institute of Technology in Rochester, NY.

WETS Processing Engineering Intern at Infineon Technologies, Richmond, VA. Worked from June, 2003 to November, 2003 as well as from June, 2004 to November, 2004 for a total of a one year.